## **FRONTIER**

# Phosphorous-substituted redox-active ligands in base metal hydrosilylation catalysis

Anuja Sharma and Ryan J. Trovitch\*

Received 00th January 20xx, Accepted 00th January 20xx

DOI: 10.1039/x0xx00000x

This article highlights the utilization of phosphine-containing redoxactive ligands for efficient hydrosilylation catalysis. Manganese, iron, cobalt, and nickel precatalysts featuring these chelates have been described and leading activities for carbonyl, carboxylate, and ester C-O bond hydrosilylation have been achieved. Mechanistic studies have provided insight into the importance of phosphine hemilability.

#### Introduction

Despite their age,  $\alpha$ -diimine (DI) and 2,6-bis(imino)pyridine (or pyridine diimine, PDI) ligands remain at the forefront of coordination chemistry. Free  $\alpha$ -diimines have been available since at least 1888,¹ and the first PDI molecules were conceived as promising tridentate ligands in the 1950s.²,³ Both ligand sets rose to prominence in the 1990s when they were found to support efficient base metal mediated olefin polymerization.⁴¹ These ligand classes are redox non-innocent and are known to accept electrons from low valent metals.⁵¹ This tendency allows first row metals to engage in reactivity that is typically associated with precious metals,¹⁰ allowing for an impressive array of organic transformations.¹¹1,1²

DI and PDI ligands are particularly effective in promoting base metal catalysed alkene and carbonyl hydrosilylation, reactions historically catalysed by precious metals  $^{13,14}$  for the synthesis of silicones and alcohols, respectively.  $^{15}$  For example, the Chirik group found that  $(^{2,6-iPr_2Ar}PDI)Fe(N_2)_2$  catalyzes alkene hydrosilylation at room temperature with turnover frequencies (TOFs) up to 364 h $^{-1}$ .  $^{16}$  This catalyst,  $(^{2,6-iPr_2Ar}PDI)Fe(CH_2SiMe_3)_2$ , and  $(^{Cy}PDI)Fe(CH_2SiMe_3)_2$  were subsequently found to catalyze aldehyde and ketone hydrosilylation at 23 °C.  $^{17}$  Ultimately, PDI catalysts  $[(^{2,6-Et_2Ar}PDI)Fe(N_2)]_2(\mu-N_2)$  and  $[(^{2,6-Me_2Ar}PDI)Fe(N_2)]_2(\mu-N_2)$  were reported to exhibit impressive alkene hydrosilylation activity at low loadings (0.004-0.03 mol%), which allowed for the ambient temperature preparation of optically transparent silicones.  $^{18}$  The utilization of bench stable  $^{2,6-iPr_2Ar}DI$  and nickel(II) 2-ethylhexanoate also allows for efficient alkene hydrosilylation

at mild temperatures (23-80 °C).  $^{19}$  Bulky DI ligands derived from acenaphthoquinone and glyoxal are known to support Fe $^{20}$  and Mn $^{21}$  catalyzed carbonyl hydrosilylation, respectively.

Notably, the aforementioned examples rely on the use of bulky 2,6-disubstituted aryl or cyclohexyl imine substituents. When we first became interested in base metal hydrosilylation catalysis, 22 our group sought to design hemilabile phosphoroussubstituted PDI and DI chelates that could provide stability to precatalysts and intermediates without inhibiting catalysis. We also desired a modular synthetic approach that allowed us to alter the length of the bridging alkylene chain and the steric or electronic properties of the phosphine substituents. In 2013, we reported that the condensation of 2,6-diacetylpyridine with 2-(diphenylphosphino)-1-ethanamine or 3-(diphenylphosphino)-1-propanamine yielded the ethylene- or propylene-bridged chelates, Ph2PEtPDI or Ph2PPrPDI (Fig. 1), respectively. 23 Schiff base condensation of 2,3-butanedione with the same amines afforded Ph2PEtDI and Ph2PPrDI, 24 and extension of this chemistry allowed us to prepare the alkyl phosphine variants iPr2PPrDI and tBu<sub>2</sub>PPrDI (Fig. 1).<sup>25</sup> This Frontier article aims to review the base metal hydrosilylation catalysis that has been achieved using these phosphine-substituted PDI and DI ligand scaffolds, while highlighting the importance of phosphine hemilability.

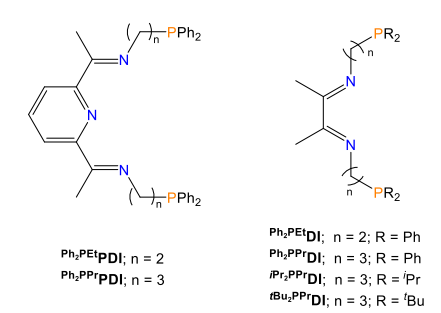


Fig. 1 Phosphorous-substituted PDI and DI ligands.

#### P-Substituted (PDI)Mn Catalysts

After confirming that Ph<sub>2</sub>PPrPDI has the ability to coordinate in a pentadentate fashion, <sup>23</sup> we sought to use it as a supporting ligand for Mn catalysis. <sup>26</sup> In 2014, (Ph<sub>2</sub>PPrPDI)Mn (1, Fig. 2) was

School of Molecular Sciences, Arizona State University, Tempe, Arizona, 85287, USA. E-mail: ryan.trovitch@asu.edu; Tel: +1 480 727 8930

COMMUNICATION Journal Name

prepared upon reducing ( $^{Ph_2PPr}PDI$ )MnCl<sub>2</sub>.<sup>27</sup> At that time, **1** was found to exhibit paramagnetically broadened and shifted  $^1H$  NMR resonances, a magnetic susceptibility of 2.2  $\mu_B$  at 23 °C, and ligand metrical parameters consistent with two electron reduction. In a subsequent study, DFT calculations revealed that the electronic structure of **1** is best described as a superposition of intermediate-spin Mn(II) antiferromagnetically coupled to a triplet PDI dianion (our preferred representation, as shown in **Fig. 2**) and low-spin Mn(II) supported by a singlet PDI dianion.<sup>28</sup>

Fig. 2 Manganese catalysts featuring a P-substituted PDI ligand.

Reacting (Ph<sub>2</sub>PPrPDI)MnCl<sub>2</sub> with 2 equiv. of NaEt<sub>3</sub>BH yielded a diamagnetic hydride complex, (Ph<sub>2</sub>PPrPDI)MnH (**2**, **Fig. 2**). Single-crystal X-ray diffraction revealed that **2** possesses a hydride-capped trigonal bipyramidal geometry and intraligand distances that are consistent with two-electron PDI reduction. While calculations supported the presence of a chelate dianion, the only suitable electronic structure for **2** was a low-spin Mn(II) center and a singlet PDI dianion, as indicated in **Fig. 2**.<sup>28</sup>

In 2017, the ethylene-bridged ligand Ph<sub>2</sub>PEtPDI was added to (THF)<sub>2</sub>MnCl<sub>2</sub> to obtain (Ph<sub>2</sub>PEtPDI)MnCl<sub>2</sub>.<sup>29</sup> Remarkably, reduction of this precursor afforded dimeric [(Ph<sub>2</sub>PEtPDI)Mn]<sub>2</sub> (**3, Fig. 2**). Single crystal X-ray diffraction revealed that each Mn center is coordinated to a κ<sup>4</sup>-PDI chelate and one neighboring PDI imine functionality. Although Ph<sub>2</sub>PEtPDI is known to coordinate in a pentadentate fashion,<sup>23</sup> **3** features one dissociated phosphine donor arm per chelate due to increased rigidity and relatively weak Mn-P bonding. The metrical parameters and EPR data collected for **3** revealed that each PDI ligand is singly-reduced and antiferromagnetically coupled to Mn(I).<sup>29</sup>

The hydrosilylation activity of **1-3** was then explored. In our 2014 report, **1** was used to hydrosilylate ketones in the presence of PhSiH<sub>3</sub> at ambient temperature.<sup>27</sup> At 1.0 mol% catalyst loading in benzene- $d_6$ , >99% conversion to a mixture of silyl ethers was achieved for 9 substrates with times ranging from 4 min to 24 h. When conducted without solvent, 0.1 mol% of **1** completely hydrosilylated acetophenone within 4 min (TOF = 248 min<sup>-1</sup>) and 0.01 mol% **1** fully hydrosilylated cyclohexanone and 2-hexanone within 5 min (TOF = 1,980 min<sup>-1</sup> based on percent conversion). Very recently, 0.01 mol% of **1** successfully hydrosilylated acetophenone and cyclohexanone within 2 min

(TOF = 4,900 min<sup>-1</sup>).<sup>30</sup> The same level of activity was noted for **1** and **2**-mediated aldehyde hydrosilylation in 2017,<sup>28</sup> and **1** was just found to catalyze benzaldehyde hydrosilylation with a TOF of 327 s<sup>-1</sup> (>98% conv. at 30 s using 0.01 mol% catalyst, believed to be the highest activity ever witnessed for carbonyl hydrosilylation).<sup>30</sup> Additionally, benzaldehyde hydrosilylation has been observed with 0.005 mol% of **3** (0.01 mol% relative to Mn) within 2 min to achieve a TOF of 9,900 min<sup>-1</sup> (4,950 min<sup>-1</sup> relative to Mn).<sup>29</sup>

Compounds **1-3** have also been used for ester and formate dihydrosilylation. In 2014, a benzene- $d_6$  solution containing 1.0 mol% of **1** and PhSiH<sub>3</sub> allowed for complete methyl acetate and ethyl acetate hydrosilylation to yield a mixture of silyl ethers after 24 h and 5.5 h, respectively.<sup>27</sup> Subsequently, 0.02-0.1 mol% of **1** and **2** were found to mediate formate hydrosilylation in the absence of solvent with TOFs of up to 330 min<sup>-1</sup>.<sup>28</sup> At time of publication, this activity was two orders of magnitude higher than the activity reported for the leading acyl C-O bond hydrosilylation catalyst.<sup>31</sup> Catalyst **3** was found to mediate formate dihydrosilylation with lower, yet still impressive, TOFs of up to 165 min<sup>-1</sup> relative to Mn.<sup>29</sup>

The mechanisms of 1 and 2 mediated hydrosilylation have been extensively studied and are known to involve phosphine dissociation and PDI redox activity.<sup>28</sup> For illustrative purposes, the mechanism of 1-catalyzed carbonyl hydrosilylation is shown in Fig. 3. First, phosphine dissociation allows for Si-H oxidative addition to generate a 5-coordinate silyl hydride intermediate that can accommodate an incoming aldehyde or ketone. Once bound, carbonyl insertion results in the formation of a silyl alkoxide intermediate that reductively eliminates the silyl ether product to regenerate 1. Notably, the oxidative addition and reductive elimination steps involve the transfer of two electrons from and to the PDI chelate, which allows Mn to remain divalent throughout the course of the reaction. Catalyst 1 can reduce sterically hindered ketones since carbonyl binding and insertion is competitive with P-arm coordination. During carboxylate dihydrosilylation, the silyl alkoxide intermediate in Fig. 3 undergoes β-alkoxide elimination prior to Si-O reductive elimination.

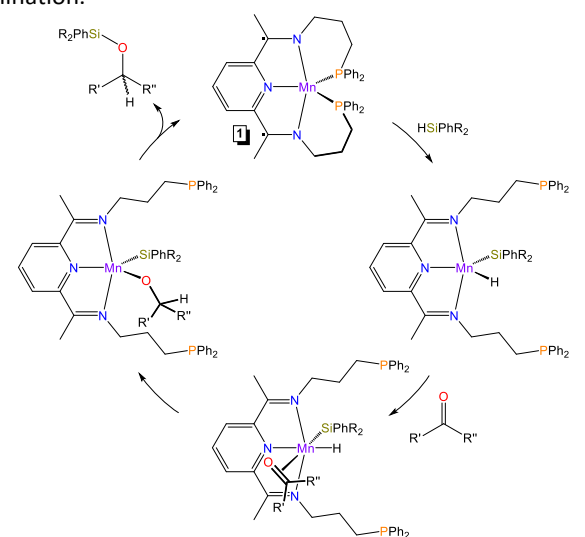


Fig. 3 Mechanism of 1-catalyzed carbonyl hydrosilylation.

Journal Name COMMUNICATION

Surprisingly, **2**-catalyzed hydrosilylation was found to occur through a different pathway. The dissociation of one phosphine arm allows for substrate binding, and insertion into the hydride results in the formation of a Mn(II) alkoxide intermediate. Then,  $\sigma$ -bond metathesis occurs upon Si-H addition to eliminate silyl ether and regenerate **2**. For formate and ester dihydrosilylation,  $\beta$ -alkoxide elimination occurs prior to Si-H  $\sigma$ -bond metathesis to release an aldehyde that is ultimately reduced. Kinetic studies revealed that the distinct mechanistic pathway used by **2** allows for more efficient formate or ester dihydrosilylation, but less efficient carbonyl hydrosilylation, relative to **1**. <sup>28</sup> Catalyst **3** was proposed to follow the same mechanisms of carbonyl and carboxylate hydrosilylation as **1** following imine dissociation to generate monomeric ( $^{\text{Ph}_2\text{PEt}}\text{PDI})\text{Mn}.^{29}$ 

### **Comparing Late First Row Metal Activity**

Knowing that P-substituted PDI ligands are highly effective at promoting Mn-based carbonyl hydrosilylation, we wondered if they would be equally useful for the preparation of Fe, Co, or Ni carbonyl hydrosilylation catalysts. Fortunately, the ability of Ph<sub>2</sub>PPrPDI to coordinate in a κ<sup>4</sup>- or κ<sup>5</sup>-fashion afforded us with an opportunity to evaluate a set of formally zerovalent compounds that increase in electron count across the first transition series.<sup>30</sup> Upon coordinating Ph<sub>2</sub>PPrPDI to FeBr<sub>2</sub> and reducing the corresponding bromide complex, we were able to prepare the Fe variant of 1, (Ph2PPrPDI)Fe (4, Fig. 4). Single crystal X-ray diffraction and computational analysis revealed that 4 features a low-spin Fe(II) center and a singlet PDI dianion. Analogously, reducing a pre-mixed solution of Ph2PPrPDI and CoCl2 yielded the Co variant,  $({}^{Ph_2PPr}PDI)$ Co (5, Fig. 4). This compound was found to possess a high-spin Co(I) center that is antiferromagnetically coupled to a PDI radical anion. Adding Ph<sub>2</sub>PPrPDI to Ni(COD)<sub>2</sub> resulted in substitution and the formation of (Ph2PPrPDI)Ni (6, Fig. 4), which features a 4-coordinate PDI chelate. Surprisingly, 6 was found to exist as a mixture of states at room temperature. The ground state triplet, which features a Ni(I) center that is uncoupled to a PDI-based radical, contributes to the 1.2  $\mu_{\text{B}}$ magnetic susceptibility observed at 25 °C. This lower than expected value for 2 unpaired electrons arises from population of the antiferromagnetically coupled singlet state, which was determined to be 1.3 kcal/mol higher in energy.

With compounds **4-6** in hand, their ability to hydrosilylate acetophenone under the conditions used for **1** was evaluated. Interestingly, **4** did not show acetophenone hydrosilylation activity when quenched with  $I_2$  after 2 min, and no conversion was noted after 24 h. However, 50% conversion was observed for this reaction when **4** was quenched in air, suggesting that the associative substitution of a phosphine donor arm with  $O_2$  activates this Fe catalyst. In contrast, **5** was found to exhibit impressive acetophenone hydrosilylation activity, with 78% conversion observed after 2 min (TOF = 3,900 min<sup>-1</sup>). Under the same conditions, **5** was found to catalyze cyclohexanone hydrosilylation with a TOF of 4,700 min<sup>-1</sup> and benzaldehyde hydrosilylation with a TOF of 4,900 min<sup>-1</sup>. At 30 s, 0.01 mol% of **5** catalyzed benzaldehyde hydrosilylation with a TOF of 223 s<sup>-1</sup>, rendering it the most active Co catalyst for carbonyl

hydrosilylation ever reported.<sup>30</sup> The Ni variant **6** was considerably less active for aldehyde and ketone hydrosilylation, with maximum turnover frequencies of 1,300 and 250 min<sup>-1</sup>, respectively.

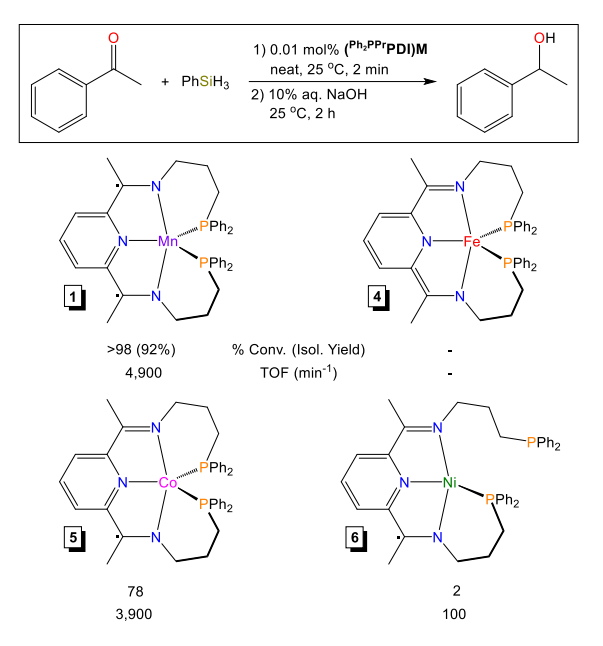


Fig. 4 Acetophenone hydrosilylation with Ph2PPrPDI compounds.

Initially, we suspected that electronic similarities between 1 and 5 were responsible for their outstanding catalytic activity. Both compounds feature a metalloradical, antiferromagnetic coupling between the remaining metal- and ligand-centered electrons, and an odd formal electron count (17 for 1 and 19 for 5, assuming the PDI electrons remain accessible). However, a thorough computational study revealed that the relative ease of phosphine arm dissociation from 1 (2.6 kcal/mol), 5 (12.4 kcal/mol), 6 (19.01 kcal/mol), and 4 (32.5 kcal/mol) is directly proportional to observed carbonyl hydrosilylation activity.<sup>30</sup>

#### P-Substituted (DI)Ni Catalysts

Phosphine hemilability has proven to be just as important for (DI)Ni hydrosilylation catalysis. The addition of Ph2PEtDI or Ph<sub>2</sub>PPrDI to Ni(COD)<sub>2</sub> afforded (Ph<sub>2</sub>PEtDI)Ni (**7, Fig. 5**) and (Ph<sub>2</sub>PPrDI)Ni (8, Fig. 5), respectively.<sup>24</sup> Structural analysis revealed that 7 has a distorted square planar geometry while 8 features a distorted tetrahedral geometry, and both complexes possess a Ni(I) center that is antiferromagnetically coupled to a DI radical synthesized the isoelectronic anion. In 2018, we trialkylphosphine complexes ('Pr2PPrDI)Ni (**9, Fig. 5**) and (tBu<sub>2</sub>PPrDI)Ni (**10**, **Fig. 5**) to fully evaluate the hydrosilylation activity (DI)Ni compounds.25

Using a 5 mol% loading, catalysts **7** and **8** were both found to mediate cyclohexanone, diisopropyl ketone, and phenyl acetylene hydrosilylation at 25 °C, but **8** was determined to be slightly more effective.<sup>24</sup> The efficiency of 1.0 mol% **8**, **9**, and **10** for benzaldehyde hydrosilylation was then assayed over the course of 3 h at 25 °C.<sup>25</sup> Complete conversion was noted for **8**,

COMMUNICATION Journal Name

while 9 and 10 afforded 8% and 67% conversion, respectively. Given its relative effectiveness, 0.1 mol% of 8 was then used to catalyze the hydrosilylation of 12 different aldehydes over the course of 24 h (Fig. 5, middle, TOF = 41 h<sup>-1</sup>). Catalyst 8 was far less active for ketone hydrosilylation (TOF = 4 h<sup>-1</sup> at 60 °C), a trend that was also observed for PDI variant 6. Moreover, 8 was found to mediate the hydrosilylation of 7 different allyl esters at 25 °C to yield propene and the respective tricarboxysilane. Notably, these trials represented the only known examples of tricarboxysilane synthesis via hydrosilylation, and repeating allyl acetate reduction with 0.1 mol% of 8 in the absence of solvent allowed for leading ester C-O bond hydrosilylation activities of up to 990 h<sup>-1</sup>.25 Compounds 9 and 10 were ineffective for allyl acetate hydrosilylation at 1.0 mol% loading, with 8% and 0% conversion noted after 30 min at 25 °C, respectively.

**Fig. 5** Nickel catalysts featuring P-substituted DI ligands (top). Reactions catalysed by **8** (middle). Mechanism of allyl ester C-O bond hydrosilylation using **8** (bottom).

Experiments were then performed to determine why  $\bf 8$  is more effective than  $\bf 9$  or  $\bf 10$  for carbonyl and allyl ester hydrosilylation. Interestingly, it was found that adding 20 equiv. of PMe<sub>3</sub> during  $\bf 8$  catalyzed benzaldehyde hydrosilylation greatly inhibited catalysis, with 3% conversion noted after 3 h at 25 °C. 25

Tracking the addition of PMe<sub>3</sub> to **8** revealed that PMe<sub>3</sub> quickly displaces the weakly-coordinated diphenylphosphine arms of  $^{Ph_2PPr}DI$ . In contrast, the trialkylphosphine arms of **9** and **10** are strongly-coordinated and inhibit carbonyl hydrosilylation by preventing silane activation and substrate coordination. Allyl ester hydrosilylation using **8** was found to proceed via olefin binding, allylic C-O bond oxidative addition,  $\sigma$ -bond metathesis, and reductive elimination (**Fig. 5**, bottom), a mechanism that is also inhibited by strong trialkylphosphine arm coordination.  $^{25}$ 

Given the activity of **8** and its ability to access alkenes, this catalyst was subsequently used to hydrosilylate terminal and *gem*-disubstituted olefins. Using  $Ph_2SiH_2$ , 1.0 mol% of **8** was found to catalyze the *anti*-Markovnikov hydrosilylation of 21 different  $\alpha$ -olefins (including allyl and vinyl ethers) over the course of 24 h at 25 °C. Ambient temperature TOFs of up to 124 h<sup>-1</sup> were recorded and heating to 60 °C allowed for alkene hydrosilylation TOFs of up to 990 h<sup>-1</sup>. Notably, **8** was also found to catalyze the hydrosilylation of 9 different *gem*-olefins over the course of 7 days at 70 °C. Although these conditions are less than ideal, this study provided the most substantial scope and highest turnover number (740) that had been reported for Nimediated *gem*-olefin hydrosilylation.  $^{32}$ 

#### **Conclusions**

The utilization of phosphine-substituted PDI and DI ligands has greatly contributed to the advancement of base metal hydrosilylation catalysis. These ligand classes have allowed for the development of a commercialized manganese catalyst that exhibits carbonyl and carboxylate hydrosilylation TOFs of up to 327 s<sup>-1</sup> and 330 min<sup>-1</sup>, respectively, as well as a commercialized nickel catalyst that exhibits ester C-O bond hydrosilylation TOFs of up to 990 h<sup>-1</sup>. At the same time, it has become clear that the incorporation of hemilabile phosphine moieties is of critical importance when developing catalysts of this type. Phosphine substituted PDI and DI ligands can help to stabilize highly-reactive base metal complexes that feature a variety of electronic structures; however, they also have the ability to inhibit substrate coordination and bond activation.

#### **Author Contributions**

A. S. is credited with investigating prior literature and writing the initial draft of this paper. R. J. T. was responsible for conceptualizing this project, acquiring funding, and editing prior to publication.

#### **Conflicts of interest**

There are no conflicts to declare.

## **Notes and references**

- 1 H. A. von Pechmann, *Ber. Deut. Chem. Ges.*, 1888, **21**, 1411-1422.
- R. C. Stoufer and D. H. Busch, J. Am. Chem. Soc., 1956, 78, 6016-6019.

Journal Name COMMUNICATION

- F. Lions and K. V. Martin, J. Am. Chem. Soc., 1957, 79, 2733-2738
- 4 L. K. Johnson, C. M. Killan and M. Brookhart, *J. Am. Chem. Soc.*, 1995, **117**, 6414-6415.
- 5 B. L. Small, M. Brookhart and A. M. A. Bennett, J. Am. Chem. Soc., 1998, 120, 4049-4050.
- 6 G. J. P. Britovsek, V. C. Gibson, B. S. Kimberley, P. J. Maddox, S. J. McTavish, G. A. Solan, A. J. P. White and D. J. Williams, Chem. Commun., 1998, 849-850.
- 7 M. G. Gardiner, G. R. Hanson, M. J. Henderson, F. C. Lee and C. L. Raston, *Inorg. Chem.*, 1994, **33**, 2456-2461.
- 8 B. de Bruin, E. Bill, B. Bothe, T. Weyhermüller and K. Wieghardt, *Inorg. Chem.*, 2000, **39**, 2936-2947.
- 9 N. Muresan, K. Chlopek, T. Weyhermüller, F. Neese and K. Wieghardt, *Inorg. Chem.*, 2007, **46**, 5327-5337.
- 10 P. J. Chirik and K. Wieghardt, Science, 2010, 327, 794-795.
- 11 M. W. Bouwkamp, A. C. Bowman, E. Lobkovsky and P. J. Chirik, *J. Am. Chem. Soc.*, 2006, **128**, 13340-13341.
- 12 P. J. Chirik, Acc. Chem. Res., 2015, 48, 1687-1695.
- 13 J. L. Speier, J. A. Webster and G. H. Barnes, *J. Am. Chem. Soc.*, 1957, **79**, 974–979.
- 14 I. Ojima, M. Nihonyanagi and Y. Nagai, *J. Chem. Soc., Chem. Commun.*, 1972, 938a.
- 15 B. Marciniec, Comprehensive Handbook on Hydrosilylation, 1<sup>st</sup> Ed., Pergamon Press, New York, USA, 1992; pp 178-217.
- 16 S. C. Bart, E. Lobkovsky and P. J. Chirik, J. Am. Chem. Soc., 2004, 126, 13794-13807.
- 17 A. M. Tondreau, E. Lobkovsky and P. J. Chirik, Org. Lett., 2008, 10, 2789-2792.
- 18 A. M. Tondreau, C. C. H. Atienza, K. J. Weller, S. A. Nye, K. M. Lewis, J. G. P. Delis and P. J. Chirik, *Science*, 2012, **335**, 567-570.
- 19 I. Pappas, S. Treacy and P. J. Chirik, ACS Catal., 2016, 6, 4105-4109.
- 20 F. S. Wekesa, R. Arias-Ugarte, L. Kong, Z. Sumner, G. P. McGovern and M. Findlater, *Organometallics*, 2015, 34, 5051-5056.
- 21 V. Yempally, A. Shahbaz, W.Y. Fan, S.T. Madrahimov and A.A. Bengali, *Inorganics*, 2020, **8**, 61.
- 22 R. J. Trovitch, Synlett, 2014, 25, 1638-1642.
- 23 H. Ben-Daat, G. B. Hall, T. L. Groy and R. J. Trovitch, Eur. J. Inorg. Chem., 2013, 4430-4442.
- 24 T. M. Porter, G. B. Hall, T. L. Groy and R. J. Trovitch., *Dalton Trans.*, 2013, 42, 14689-14692.
- 25 C. L. Rock, T. L. Groy and R. J. Trovitch, *Dalton Trans.*, 2018, **47**, 8807-8816.
- 26 R. J. Trovitch, Acc. Chem. Res., 2017, 50, 2842-2852.
- 27 T. K. Mukhopadhyay, M. Flores, T. L. Groy and R. J. Trovitch, J. Am. Chem. Soc., 2014, 136, 882-885.
- 28 T. K. Mukhopadhyay, C. L. Rock, M. Hong, D. C. Ashley, T. L. Groy, M.-H. Baik and R. J. Trovitch, J. Am. Chem. Soc., 2017, 139, 4901-4915.
- 29 T. K. Mukhopadhyay, C. Ghosh, M. Flores, T. L. Groy and R. J. Trovitch, *Organometallics*, 2017, **36**, 3477-3483.
- 30 M. R. Mena, J.-H. Kim, S. So, H. Ben-Daat, T. M. Porter, C. Ghosh, A. Sharma, M. Flores, T. L. Groy, M.-H. Baik and R. J. Trovitch, *J. Am. Chem. Soc.* (under review).
- 31 A. J. Ruddy, C. M. Kelly, S. M. Crawford, C. A. Wheaton, O. L. Sydora, B. L. Small, M. Stradiotto and L. Turculet, *Organometallics*, 2013, **32**, 5581-5588.
- 32 C. L. Rock and R. J. Trovitch, *Dalton Trans.*, 2019, **48**, 461-467.